BMC Biochemistry

Research article

Open Access

Probing the interface in a human co-chaperonin heptamer: residues disrupting oligomeric unfolded state identified

Jesse J Guidry[1], Frank Shewmaker[1], Karol Maskos[2], Samuel Landry[3] and Pernilla Wittung-Stafshede*[1]

Address: [1]Chemistry Department, Tulane University, New Orleans, 70118 Louisiana, USA, [2]Coordinated Instrumentation Facility, Tulane University, New Orleans, 70118 Louisiana, USA and [3]Biochemistry Department, Tulane University, New Orleans, 70112 Louisiana, USA

Email: Jesse J Guidry - guidry@tulane.edu; Frank Shewmaker - fshewma@tulane.edu; Karol Maskos - maskos@tulane.edu; Samuel Landry - landry@tulane.edu; Pernilla Wittung-Stafshede* - pernilla@tulane.edu

* Corresponding author

Published: 02 October 2003

BMC Biochemistry 2003, **4**:14

Received: 01 July 2003
Accepted: 02 October 2003

This article is available from: http://www.biomedcentral.com/1471-2091/4/14

© 2003 Guidry et al; licensee BioMed Central Ltd. This is an Open Access article: verbatim copying and redistribution of this article are permitted in all media for any purpose, provided this notice is preserved along with the article's original URL.

Abstract

Background: The co-chaperonin protein 10 (cpn10) assists cpn60 in the folding of nonnative polypeptides in a wide range of organisms. All known cpn10 molecules are heptamers of seven identical subunits that are linked together by β-strand interactions at a large and flexible interface. Unfolding of human mitochondrial cpn10 in urea results in an unfolded heptameric state whereas GuHCl additions result in unfolded monomers. To address the role of specific interface residues in the assembly of cpn10 we prepared two point-mutated variants, in each case removing a hydrophobic residue positioned at the subunit-subunit interface.

Results: Replacing valine-100 with a glycine (Val100Gly cpn10) results in a wild-type-like protein with seven-fold symmetry although the thermodynamic stability is decreased and the unfolding processes in urea and GuHCl both result in unfolded monomers. In sharp contrast, replacing phenylalanine-8 with a glycine (Phe8Gly cpn10) results in a protein that has lost the ability to assemble. Instead, this protein exists mostly as unfolded monomers.

Conclusions: We conclude that valine-100 is a residue important to adopt an oligomeric unfolded state but it does not affect the ability to assemble in the folded state. In contrast, phenylalanine-8 is required for both heptamer assembly and monomer folding and therefore this mutation results in unfolded monomers at physiological conditions. Despite the plasticity and large size of the cpn10 interface, our observations show that isolated interface residues can be crucial for both the retention of a heptameric unfolded structure and for subunit folding.

Background

Protein-protein interactions are of fundamental importance to molecular biology because they determine a wide array of protein structures and functions. In addition to heterogeneous protein-protein complexes, many proteins are oligomeric due to the association of identical subunits. In fact, the majority, 70–80 %, of all enzymes are oligomeric [1]. The function of quaternary structure, i.e. the arrangement of multiple subunits into an oligomer, may be to allow for cooperative effects, formation of novel active sites, provide additional stability, increase solubility or decrease osmotic pressure [2]. The folding pathways of only a few oligomeric proteins (mostly dimers and tetramers) have been reported, revealing a variety of

mechanisms [3–7]. Some proteins display monomeric or dimeric intermediates (e.g. *E. coli* Trp repressor and the ATPase SecA [8,9]) whereas other fold in apparent two-state reactions in which folding and oligomerization are coupled (e.g. P22 Arc repressor [10,11]). It remains a challenge to understand the way in which the amino acid sequence of a polypeptide controls both the folding of individual subunits and their assembly to higher-order quaternary structures.

The heptameric co-chaperonin protein 10 (cpn10) is an attractive model for studies of the interplay between polypeptide folding and protein-protein assembly. The primary function of the cpn10 heptamer is to assist cpn60 in folding of nonnative proteins. Upon binding to cpn60, cpn10 forms a cap covering the central cavity of cpn60, and folding of substrates (nonnative proteins) is achieved through cycles of ATP-dependent binding and dissociation [12–15]. The quaternary structures of the cpn10 and cpn60 proteins appear conserved in all organisms. In addition to the well-established co-chaperonin activity, several cpn10 proteins are potent stimulators of the immune system. Despite that their structural homology, there are dramatic immunogenic differences between cpn10 proteins from different species: for instance, human and *E. coli* cpn10 are very poor immunogens whereas *Mycobacterium tuberculosis* and *Mycobacterium leprae* are strong immunogens [16,17]. Co-chaperonin proteins can also stimulate T lymphocyte proliferation, induce cytokine secretion, trigger apoptosis, and affect cell growth and development [18]. It is not known what oligomeric or structural states of the cpn10 proteins are used to promote these additional, non-chaperonin functions.

Cpn10 from *E. coli*, GroES, is the most thoroughly studied co-chaperonin protein and a crystal structure has been described [19]. Crystal structures for *Mycobacterium tuberculosis* and *Mycobacterium leprae* cpn10 and bacteriophage T4 Gp31 proteins have also been reported [20–22]. Each *E. coli* cpn10 subunit adopts an irregular β-barrel topology. The dominant interaction between the subunits in the native doughnut-like structure is an anti-parallel pairing of the first β-strand in one subunit and the final β-strand in the other subunit [19]. The core residues of these strands are conserved among cpn10 proteins. According to the crystal structure of *E. coli* cpn10, there are also many additional, complementary interactions that stretch across the interface. The flexibility of the involved side chains, and of the backbone in these regions, contributes to the plasticity of the interface. Human mitochondrial cpn10 is 37 % identical to GroES in terms of primary structure. X-ray crystallography and NMR spectroscopy studies have revealed human cpn10 to have a fold, with similar flexible regions, that is identical to the fold of *E. coli* GroES [23–25].

We recently showed that human cpn10 dissociates into monomers below a concentration of approximately 3 μM (monomer concentration), corresponding to a ΔG_{diss} of 195 kJ/mol, heptamer [26]. This modest affinity might be linked to a significant loss of configurational entropy upon oligomerization, which would be the case if folding and assembly processes are coupled. In accord, we have found that monomeric cpn10 adopts a folded structure in solution, but that it exhibits only marginal thermodynamic stability [27]. Chemically-induced unfolding using GuHCl leads to a monomeric unfolded state whereas, interestingly, non-native heptamers form when using urea as the denaturant [26]. Thermally- and chemically-induced unfolding reactions of cpn10 are fully reversible: during the equilibrium unfolding processes no other oligomeric species, except for heptamers and monomers, have been observed [26]. From a biophysical point of view, it is remarkable that the cpn10 polypeptides adopt the unique heptameric structure without any misfolding, misassembly, or aggregation side reactions.

To begin to identify the role of interfacing residues for adopting the oligomeric structure, we designed two point-mutated variants of human mitochondrial cpn10. In one variant, a valine in the final β-strand has been replaced by glycine (Val100Gly cpn10), in the other, a phenylalanine in the N-terminal β-strand has been replaced by a glycine (Phe8Gly cpn10) (Figure 1). The biophysical behaviors of the two cpn10 variants are dramatically different. The folded state of Val100Gly cpn10 remains heptameric although it exhibits somewhat lower thermodynamic stability as compared to wild-type cpn10. This mutation, however, disrupts the unfolded oligomeric state found for wild-type cpn10 in urea. In the case of Phe8Gly cpn10, this mutation both unfolds the protein and dissociates the heptamer into mostly monomers. We conclude that despite the large and plastic subunit-subunit interface, a specific residue, like the highly conserved phenylalanine-8, can have a crucial role for both assembly of cpn10 in the unfolded state and for the folding and assembly of each subunit in the native state. Other interfacial residues, such as the non-conserved valine-100, have only modest effects on the folding of the subunits and the native oligomeric state, but still significant effects on the unfolded quaternary structure of cpn10.

Results

Oligomeric state of cpn10 variants

The quaternary structure of Val100Gly and Phe8Gly cpn10 variants were probed by gluteraldehyde cross-linking as well as by gel-filtration under native conditions (5 mM phosphate, pH 7, 20°C). Val100Gly cpn10 forms heptamers, like wild-type cpn10, according to both cross-linking and gel-filtration experiments (Figure 2A and 2B). In contrast, cross-linking results suggest that Phe8Gly

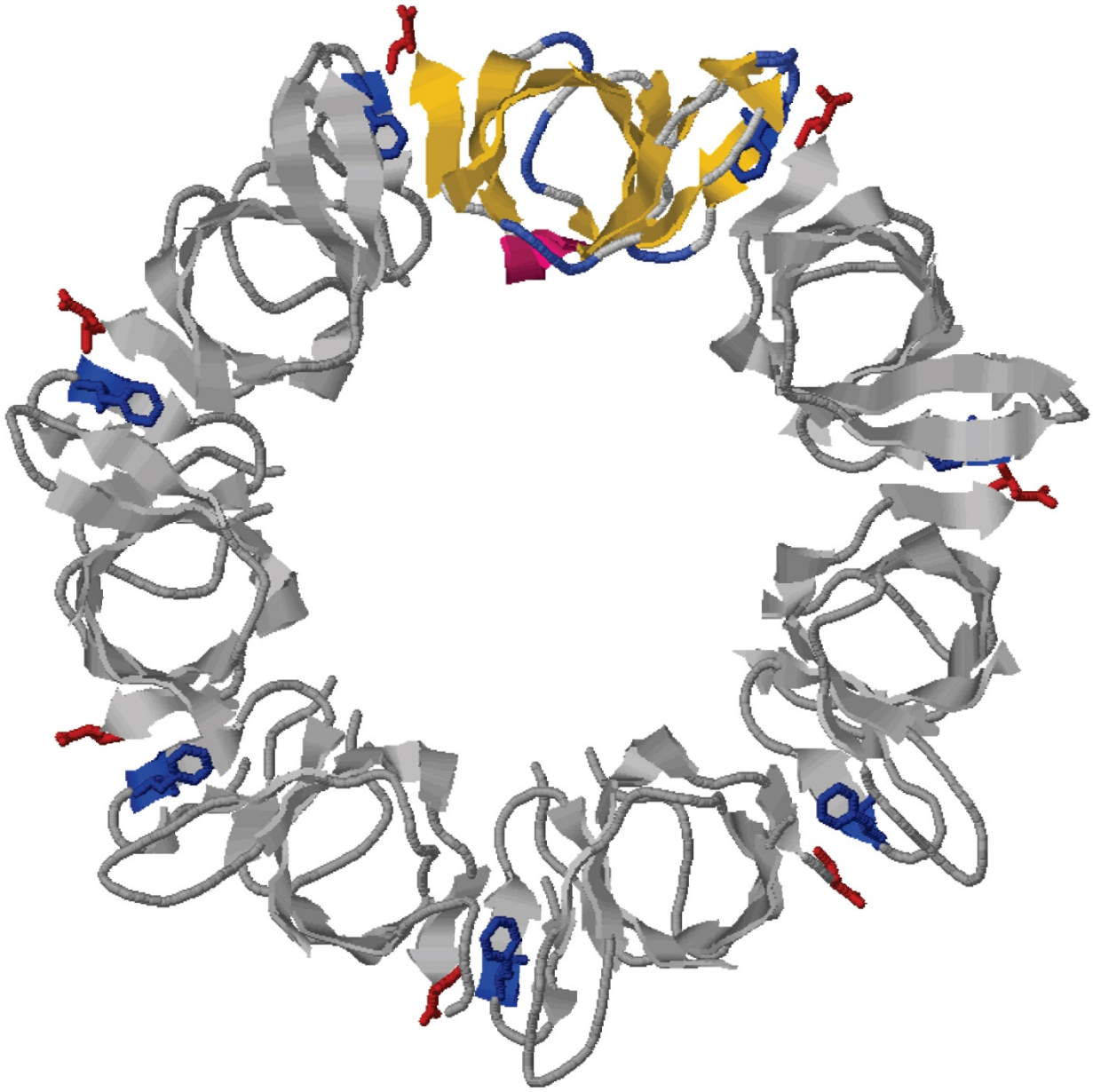

Figure 1
Structure of heptameric human mitochondrial cpn10 [23] with Phe8 (blue) and Val100 (red) highlighted in all subunits. One monomer is highlighted in yellow. Diagram produced in RasWin v2.6.

cpn10 forms an array of monomeric, dimeric, trimeric, etc. species, with monomers and dimers dominating, at protein concentrations up to 1 mM monomer concentration (Fig. 2A). In addition, gel-filtration on Phe8Gly cpn10 suggests the presence of oligomeric species with sizes in between that of dimers and trimers (Fig. 2B).

Secondary and tertiary structure of cpn10 variants

The far-UV CD signal of Val100Gly cpn10 is identical to that of wild-type cpn10 in agreement with folded, β-barrel subunits forming the heptameric ring (Figure 3A). In addition, tyrosine fluorescence of Val100Gly cpn10 indicates a folded, native-like species (Figure 3B). ANS binds

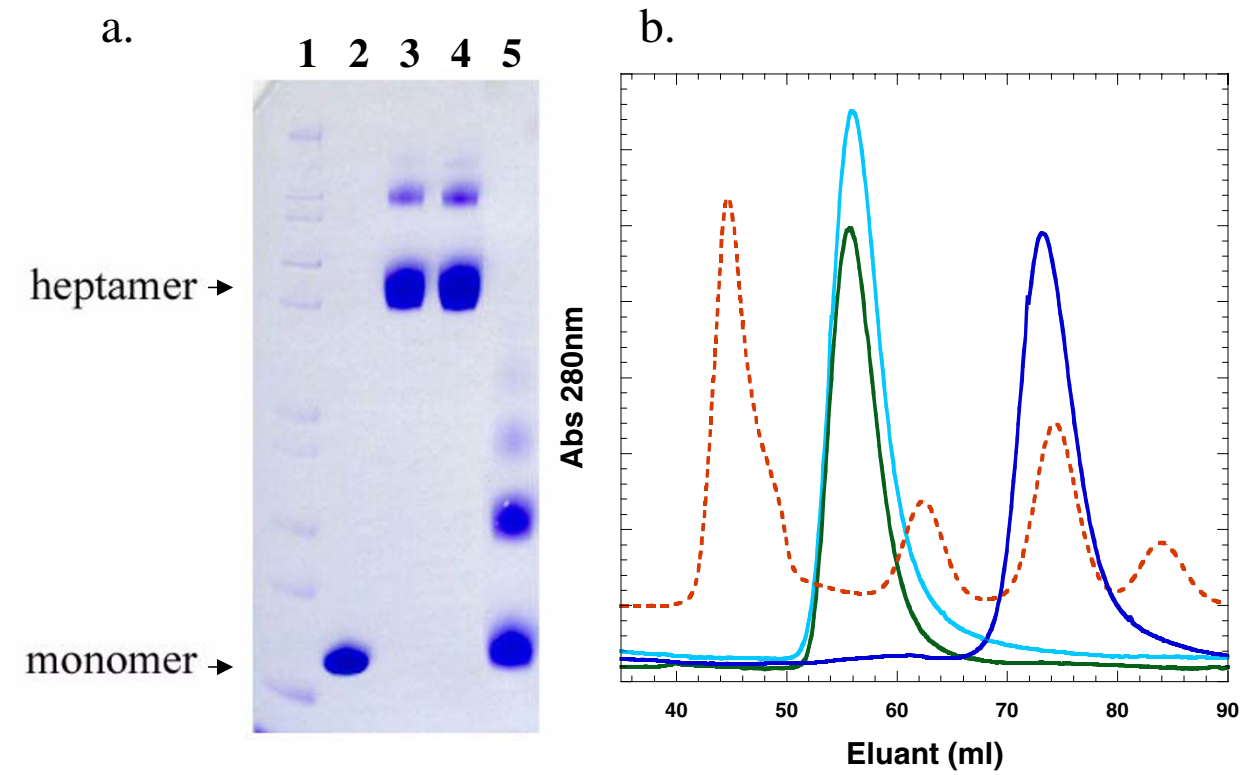

Figure 2
A. Polyacrylamide gel showing cpn10 variants after treatment with cross-linking agent gluteraldehyde (lanes 3–5). All reactions included 60 μM total protein (5 μg total protein loaded in each lane). Lane 1, marker (200.0 kDa; 116.0 kDa; 97.4 kDa; 66.3 kDa; 55.4 kDa; 36.5 kDa; 31.0 kDa, 21.5 kDa; 14.4 kDa; 6.0 kDa); Lane 2, wild-type cpn10 without cross-linking agent; Lane 3, wild-type cpn10; Lane 4, Val100Gly cpn10; Lane 5, Phe8Gly cpn10. B. Gel filtration traces for wild-type cpn10 (light blue), Val100Gly cpn10 (green), and Phe8Gly cpn10 (blue). The column was calibrated with molecular weight globular standards (dashed line): Ribonuclease A, 13,700 Da; Chymotrypsinogen A, 25,000 Da; Ovalbumin, 43,000 Da; Bovine Serum Albumin, 67,000 Da; Blue Dextran 2000, » 2,000,000 Da.

to hydrophobic exposed surfaces and its increased emission upon such binding has been used extensively to probe non-native, intermediate states of proteins [29–32]. In accord with a well-folded structure, we find no increase in ANS emission in the presence of Val100Gly cpn10 as compared to in the presence of wild-type cpn10 (data not shown).

In sharp contrast, Phe8Gly cpn10 does not adopt native tertiary structure since the characteristic tyrosine contribution at 230 nm in the far-UV CD spectrum, reporting on the restricted environment of the three tyrosines [26], is absent (Figure 3A). Moreover, the tyrosine emission of Phe8Gly cpn10 is similar to that of unfolded wild-type cpn10 (Figure 3B). Still, Phe8Gly cpn10 exhibits some residual secondary structure according to far-UV CD (Figure 3A).

To further address the presence of structure in the Phe8Gly cpn10 variant, one-dimensional NMR data was collected. ^{1}Hα shifts are reliable predictors of backbone dihedral angles and secondary structure [33]. Figure 4A,4B,4C,4D shows the 11.0 ppm to 3.35 ppm region of the ^{1}H spectra recorded at 25 °C of wild-type cpn10 at pH 7 (A) and pH 3 (B) and Phe8Gly cpn10 at pH 7 (C) and pH 3 (D). The spectra of both molecules at pH 7 look similar: the broad amide resonances are dispersed downfield up to ~10 ppm and some α protons are resonating downfield from the water signal up to 5.7 ppm. The similarity of these two spectra indicates that some secondary structure is still retained in Phe8Gly cpn10 at pH 7. However, drastically different spectra were recorded after lowering the pH. The wild-type cpn10 spectrum at pH 3 (Fig. 4B) has not changed much. However, in the Phe8Gly cpn10 spectrum at pH 3 (Fig. 4D) the sharp amide protons

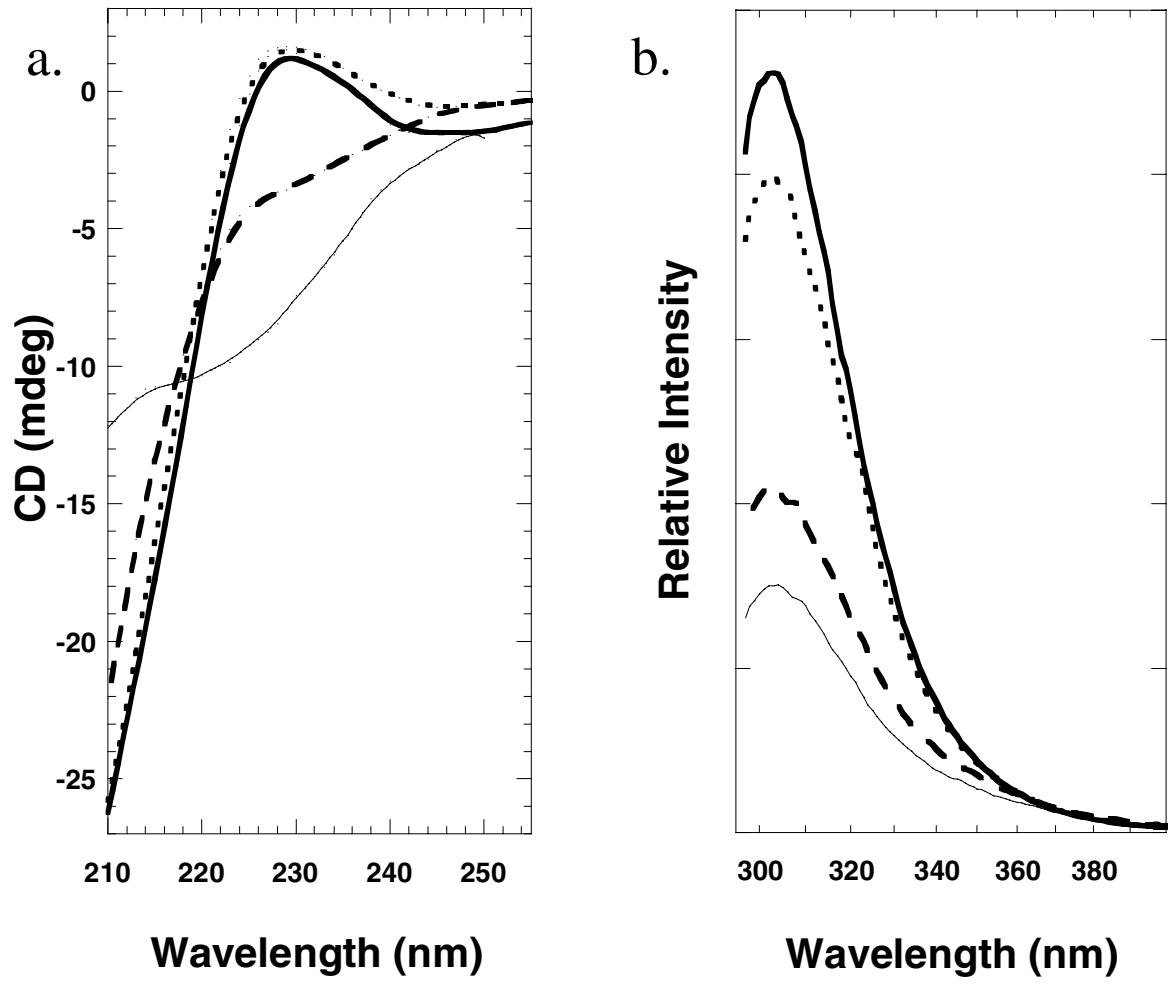

Figure 3
A. Far-UV CD spectra of wild-type cpn10 (solid line), Val100Gly cpn10 (dotted line), and Phe8Gly cpn10 (dashed line) in 5 mM phosphate, pH 7 (20°C). Also shown is unfolded wild-type cpn10 (thin line) in 4 M GuHCl (pH 7, 20°C). B. Tyrosine emission (excitation 280 nm) of wild-type cpn10 (solid line), Val100Gly cpn10 (dotted line), and Phe8Gly cpn10 (dashed line) in 5 mM phosphate, pH 7 (20°C). Also shown is unfolded wild-type cpn10 (thin line) in 4 M GuHCl (pH 7, 20°C).

resonate in the narrow 8.0–8.7 ppm region and none of the α protons is visible downfield from 4.7 ppm, clearly indicating that at this pH Phe8Gly cpn10 exists in a fully unfolded state. Taken together, the NMR data shows that Phe8Gly cpn10 adopts some secondary structure at pH 7, but that these structural elements are not stable.

There is an increase in ANS emission (5-fold as compared to wild-type and Val100Gly cpn10 variants) when in presence of Phe8Gly cpn10 at pH 7. This supports that this variant is not correctly folded but has exposed hydrophobic surfaces.

Thermal denaturation of Val100Gly cpn10 variant

Thermal unfolding of wild-type cpn10 leads to unfolding and dissociation and, therefore, there is a protein-concentration dependence in the transition midpoints (T_m): the higher the protein concentration, the higher the T_m [26]. Thermal unfolding of wild-type and Val100Gly cpn10 can be monitored by changes in far-UV CD and tyrosine emission, as well as by differential scanning calorimetry (DSC). Regardless of the probing method, the thermal midpoint is the same for a particular protein concentration, suggesting that thermal denaturation is an apparent two-state mechanism with only folded heptamers and unfolded monomers involved (data not shown). The T_m

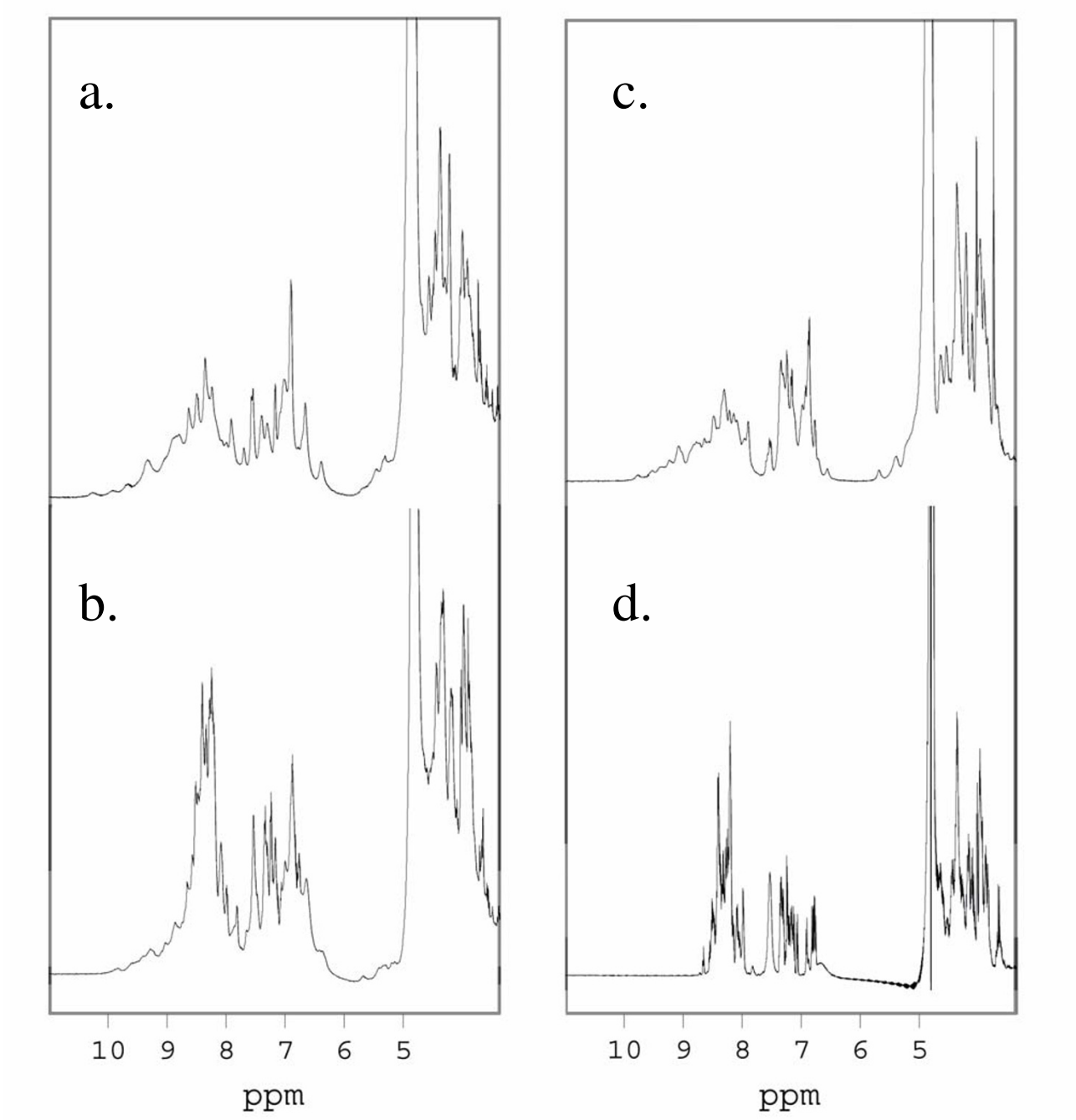

Figure 4
Comparison of ^{1}H resonances dispersion (11.0 ppm to 3.35 ppm) in wild-type cpn10 (A, pH 7 and B, pH 3) and Phe8Gly cpn10 (C, pH 7 and D, pH 3) at 25°C.

values are lower for the Val100Gly mutant as compared to those for wild-type cpn10 (for identical total protein concentrations), in accord with a decrease in monomer stability and/or subunit-subunit binding affinity in Val100Gly cpn10 (Figure 5A, Table 1). The breakpoint of the T_m versus protein concentration graph indicates a heptamer-to-monomer Kd of ~5 μM for Val100Gly cpn10 (corresponding to a ΔG_{diss} of ~185 kJ per mol of heptamer). This value

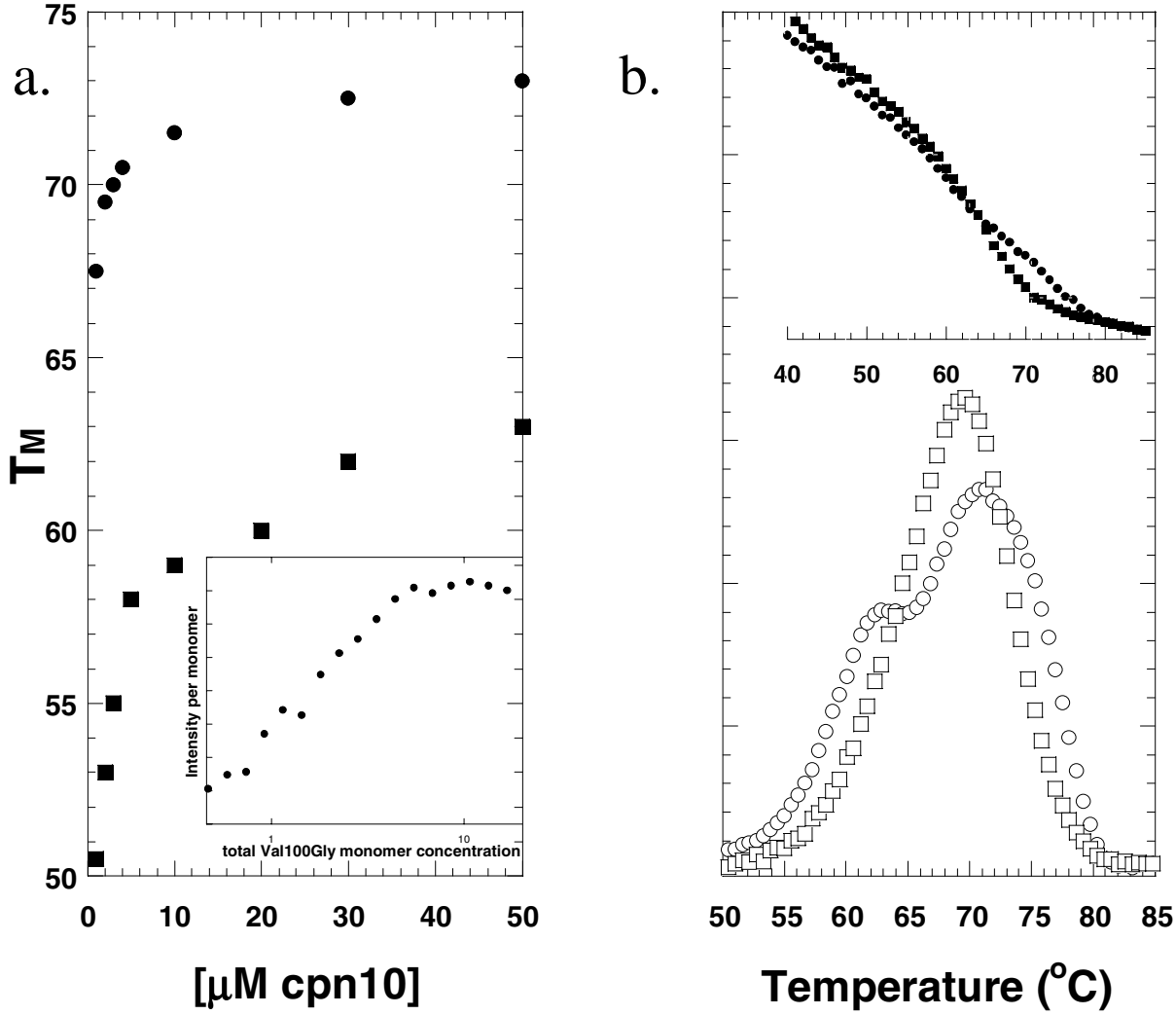

Figure 5
A. Thermal midpoints (T_m) as a function of cpn10 (total monomer) concentration (5 mM phosphate, pH 7); wild-type cpn10 (circles) and Val100Gly cpn10 (squares). Inset: Relative fluorescence (308 nm) per Val100Gly cpn10 monomer as a function of total concentration. B. DSC thermograms for 1st (open circles; T_ms of 63°C and 72.5°C) and 2nd (open squares; T_m of 69°C) thermal scans after mixing 40 μM Val100Gly cpn10 with 40 μM wild-type cpn10 at 20°C (5 mM phosphate, pH 7). Top: Relative fluorescence changes for 1st (filled circles; Tms of 59°C and 71.5°C) and 2nd (filled squares; Tm of 65°C) thermal scans after mixing 9 μM Val100Gly cpn10 with 12 μM wild-type cpn10 at 20°C (5 mM phosphate, pH 7).

is further supported by dilution experiments monitoring tyrosine fluorescence as a function of protein concentration (Inset, Figure 5A), a method previously used to probe the K_d [26].

Interaction of cpn10 variants with wild-type cpn10

Both cpn10 variants were tested for their ability to substitute as subunits in the wild-type cpn10 heptamer using thermal denaturation as the detection probe. Each mutant was mixed with wild-type cpn10 in various mixing ratios and thermal transitions were monitored by both tyrosine fluorescence and DSC. In all cases, the first thermal scans resulted in two transitions, corresponding to each protein's individual thermal transition, suggesting that at room temperature the cpn10 heptamers do not exchange

Table 1: Thermal midpoints (T_m) observed with different Val100Gly and wild-type cpn10 total protein (monomer) concentrations (5 mM phosphate, pH 7). Error bar is ± 1°C in each case.

Protein concentration (μM)	T_m (°C) Val100Gly cpn10	T_m (°C) wild-type cpn10
1	50.5	67.5
2	53	69.5
3	55	70
4	-	70.5
5	58	-
10	59	71.5
20	60	-
30	62	72.5
50	63	73

subunits with other heptamers (or other oligomers in the case of mixing with Phe8Gly cpn10).

When Val100Gly cpn10 was mixed with wild-type cpn10, the second scans (i.e. after one cycle of heating and cooling) revealed single thermal transitions with midpoints in between the two individual T_m values (examples in Figure 5B). The second-scan T_m values depended linearly on the mixing ratio of Val100Gly to wild-type cpn10 (data not shown), as would be the case if the two cpn10 monomers mix and form new hybrid heptamers upon cooling according to the stoichiometry of monomers in solution. This finding strongly support that Val100Gly cpn10 forms native-like oligomers.

In stark contrast, second scans of Phe8Gly cpn10 mixed with wild-type cpn10 did not differ from the first thermal scans (data not shown). Second scans, again, showed a broad low T_m of Phe8Gly cpn10 (at ~40°C) and a higher more cooperative T_m for wild-type cpn10. Thus, even upon dissociation and unfolding, wild-type cpn10 subunits do not interact with Phe8Gly cpn10 subunits. One would expect a native-like Phe8Gly cpn10 monomer to have the ability to pair with at least one wild-type cpn10 monomer (C-terminus side of Phe8Gly cpn10 is not altered). Since no interactions are observed at all, this further supports that Phe8Gly cpn10 is mostly unfolded.

Ability of cpn10 variants to assist in substrate refolding

The functional consequence of the two cpn10 mutations was tested in a GroEL-dependent citrate synthase refolding assay *in vitro*. In our set up (see Methods), the presence of wild-type cpn10 results in GroEL-assisted refolding of citrate synthase to 52 ± 4 %. This amount is similar to GroEL-assisted refolding of citrate synthase in the presence of GroES [26]. Presence of the Val100Gly cpn10 variant resulted in substrate refolding as efficient, or slightly better, than wild-type cpn10 (62 ± 4 % citrate synthase refolding). The Phe8Gly cpn10 variant, however, failed to assist GroEL in substrate refolding (< 3 % citrate synthase refolding).

GuHCl and urea-induced denaturation of Val100Gly cpn10

Previously we have shown (surprisingly) that the denatured state at room temperature of wild-type cpn10 strongly depends on the chaotropic agent used, urea or GuHCl [26]. In equilibrium-unfolding experiments using GuHCl, wild-type heptameric cpn10 dissociates and unfolds in a coupled, apparent two-state (folded heptamers to unfolded monomers), process, while urea promotes unfolding but not dissociation of the cpn10 structure (folded heptamers to unfolded, or non-native, heptamers). We find that also with Val100Gly cpn10, the nature of the chemical denaturant affects the unfolding/dissociation mechanism although the final state reached is always that of unfolded monomers. Upon additions of GuHCl, far-UV CD and tyrosine emission signals of Val100Gly cpn10 change simultaneously in a two-state like reaction. Independent of Val100Gly cpn10 concentration, the equilibrium-unfolding transition midpoint occurs at ~0.7 M GuHCl (Figure 6A, Table 2). Correlating cross-linking experiments of identical Val100Gly/GuHCl samples reveal that this cpn10 variant is heptameric during the far-UV CD and fluorescence transition, and that the monomeric species is not detected until after around 1 M GuHCl has been added (data not shown). Thus, Val100Gly cpn10 denaturation induced by GuHCl is a three-state process: polypeptide unfolding occurs at low GuHCl concentrations (detected by fluorescence and far-UV CD) and is followed by oligomer disassembly (as observed by cross-linking) at higher GuHCl concentrations. From Figure 6A, we derive the free energy of heptamer unfolding without dissociation (i.e. two-state analysis of the first step: from folded to non-native heptamer) to around 12 kJ per mol of heptamer (Table 2). This corresponds to a predicted $\Delta G_U(H_2O)$ of ~1.7 kJ per mol of monomer.

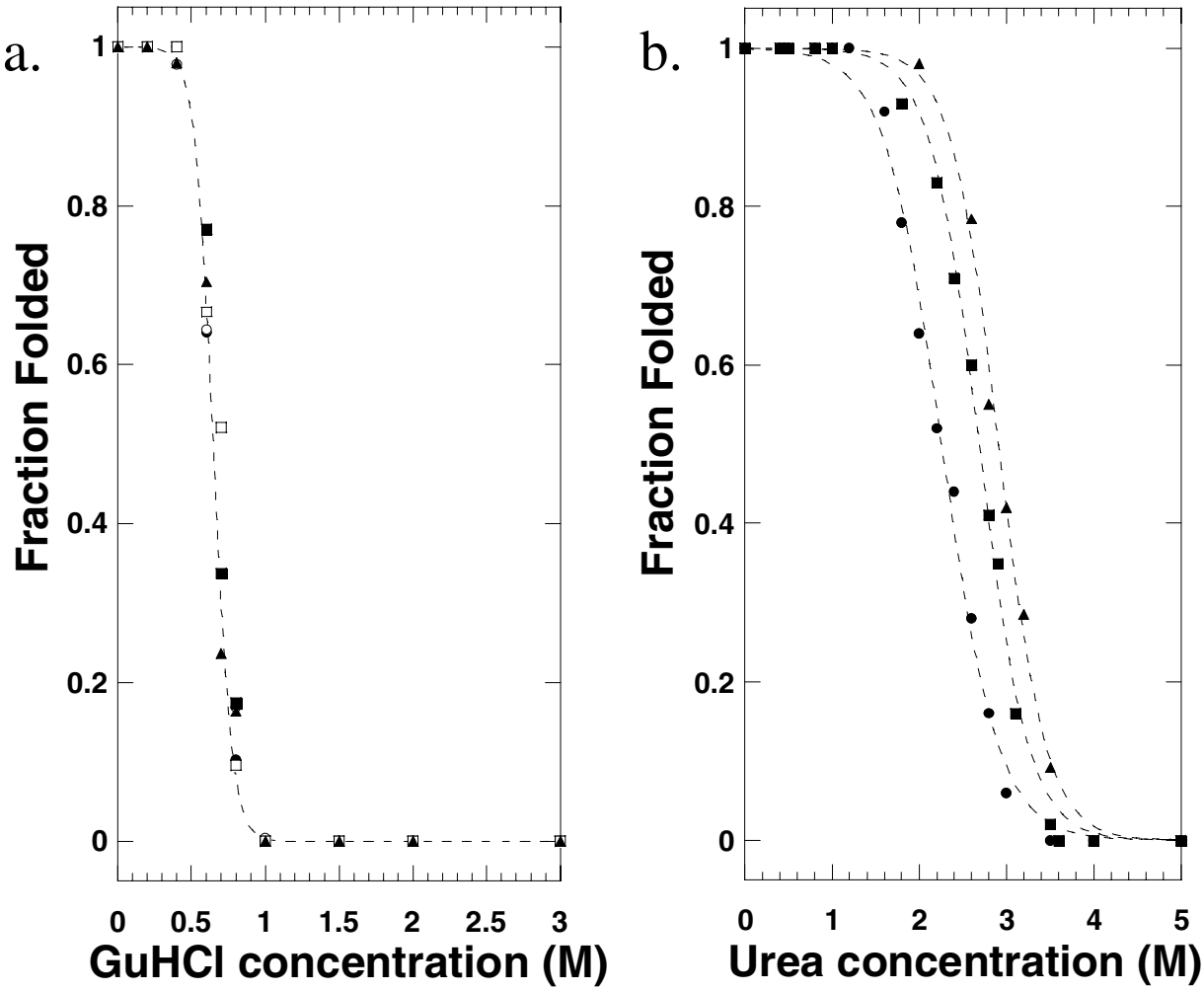

Figure 6
A. GuHCl-induced unfolding of Val100Gly cpn10 (pH 7, 20°C) monitored by fluorescence (solid symbols) and CD (open symbols) at various total protein concentrations; 30 μM (circles), 50 μM (squares), and 70 μM (triangles). B. Urea-induced unfolding of Val100Gly cpn10 (pH 7, 20°C) monitored by fluorescence changes at 308 nm at various total protein concentrations; 30 μM (circles), 50 μM (squares), and 70 μM (triangles). Far-UV CD measurements give identical transitions.

When urea is used as the chemical denaturant, the equilibrium-unfolding mechanism for Val100Gly cpn10 is different from that of Val100Gly cpn10 in GuHCl and from that of wild-type cpn10 in urea. A protein-concentration dependence is observed in the urea-induced data as monitored by spectroscopy: the more protein present, the more stable appears the heptamer (Figure 6B, Table 2). This can be explained by an apparent two-state mechanism in which only folded heptamers and unfolded monomers are populated. Thus, the valine-100 mutation abolishes the ability of cpn10 to adopt an unfolded oligomeric structure in urea. Using a 1-folded heptamer to 7-unfolded monomers mechanism to analyze the unfolding data in Figure 6B, a free energy for going from a folded Val100Gly heptamer to seven unfolded monomers of 197 kJ/mol heptamer is estimated (Table 2). In Figure 7, a simple scheme for unfolding and disassembly pathways of the cpn10 heptamer (wild-type and Val100Gly variants) is shown.

Table 2: Thermodynamic parameters (denaturant concentrations at transition midpoints and corresponding free energies extrapolated to zero denaturant concentration) for Val100Gly cpn10 denaturation by GuHCl and urea (pH 7, 20°C) at various total protein concentration.

Denaturant	[protein] (μM)	Midpoint (M)	$\Delta GU(H_2O)$ (kJ/mol oligomer)	$\Delta GU(H_2O)$ average (kJ/mol oligomer)
GuHCl[a]	10	0.7	10 ± 1	
	30	0.7	14 ± 1	
	50	0.7	11 ± 2	12 ± 2
Urea[b]	30	2.25	197 ± 6	
	50	2.70	195 ± 6	
	70	3.00	200 ± 6	197 ± 6

a. $\Delta GU(H_2O)$ calculated using a 7-mer to 7-mer reaction mechanism. b. $\Delta GU(H_2O)$ calculated using a 7-mer to 1-mer reaction mechanism.

Discussion

Cpn10 is a heptamer of seven identical subunits forming a ring-structure of seven-fold symmetry. β-strand pairing between the N-terminus of one subunit and the C-terminus of another is the major source of interactions in the rather large and flexible subunit-subunit interface [23]. In context of such plasticity, how can heptamer specificity be achieved? To begin to address this question, we used the crystal structure of human mitochondrial cpn10 [23] to design two point-mutated variants. Valine-100 is situated at the end of the C-terminal β-strand (residues 92–100) that pairs with the N-terminal β-strand (residues 7–13) at the subunit-subunit interface in human cpn10. According to the crystal structure, this residue makes close contact with Lys-7 and Leu-9 in the neighboring subunit. The other selected residue, phenylalanine-8, interacts with residues leucine-9 and proline-10 intra-molecularly, and leucine-96 to tyrosine-99 inter-molecularly.

Our biophysical characterization shows that replacing valine-100 with glycine (Val100Gly cpn10) results in a wild-type-like heptameric protein with wild-type-like function, although the overall thermodynamic stability of the heptamer is decreased. Like wild-type cpn10, the unfolding/dissociation mechanism for Val100Gly cpn10 depends on the chemical denaturant; however the mechanisms in urea and GuHCl differ from those determined for wild-type cpn10: importantly, an unfolded heptameric state is never stable (Figure 7). In urea, wild-type cpn10 unfolds to a non-native heptamer [26]. Val100Gly cpn10, on the other hand, unfolds in an apparent two-state reaction from folded heptamers to unfolded monomers in urea. This can be explained by a crucial destabilization of the interface interactions in the unfolded mutant. In GuHCl, which is a stronger denaturant, wild-type cpn10 unfolds by an apparent two-state mechanism with only folded heptamers and unfolded monomers populated. GuHCl additions to Val100Gly cpn10 also result in unfolded monomers, although here a non-native heptamer is detected as an intermediate along the path. This implies that the mutation must have an effect on monomer stability as well as on the interface stability; in fact, the destabilization of the folded monomer must be larger than any destabilization of the interface in the folded state. This is supported by the thermodynamic parameters presented in Figure 7. Comparing the K_{diss} for heptamer dissociation of wild-type and Val100Gly cpn10 shows that the folded interface in Val100Gly cpn10 is destabilized by only ~5 %, whereas the stability of the folded monomer is destabilized by ~45 % as compared to wild-type cpn10. It is clear that valine-100, although situated on the interface, plays a role for the stability of the folded monomeric unit. In accord, valine-100 packs with Tyr-99 on the surface of the β-barrel [23] and upon its removal a destabilizing solvent channel towards the hydrophobic core may be created.

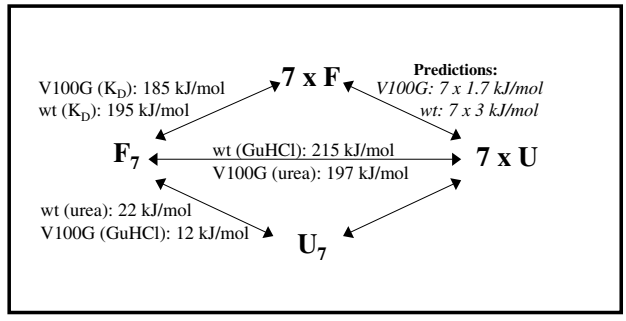

Figure 7
Thermodynamic scheme for unfolding (F, folded; U, unfolded) and disassembly (index 7, heptamer; no index, monomer) of Val100Gly (V100G) and wild-type (wt) cpn10. Energetics, calculated from KD determinations and chemical-denaturant unfolding reactions, are shown together with the derived predictions for unfolding of monomers. See text for further discussion.

Table 3: A. Protein sequence alignment of cpn10 N- and C-terminal strands involved in subunit-subunit interactions. Mutated human cpn10 residues discussed in this paper are underlined.

A. Sequence Name	N-terminus	C-terminus
CH10_MYCLE	KIKPLEDK...	...ARDVLAVVS
CH10_MYCTU	NIKPLEDK...	...ARDVLAVVS
CH10_ECOLI	NIRPLHDR...	...ESDILAIVE
CH10_MOUSE	KFLPLFDR...	...DSDILGKYV
CH10_YEAST	SIVPLMDR...	...DAEILAKIA
CH10_RAT	KFLPLFDR...	...DGDILGKYV
CH10_HUMAN	K<u>E</u>LPLFDR...	...DGDILGKY<u>V</u>

In sharp contrast to the findings on Val100Gly cpn10, upon eliminating phenylalanine-8, the heptamer never assembles and the monomers are mostly unfolded (and do not function in substrate refolding together with GroES). The phenylalanine-8 mutation thus disrupts the ability of cpn10 to fold and assemble, and it also abolishes the ability to adopt an unfolded oligomeric state. Our Phe8Gly cpn10 observations imply that either correct assembly is a prerequisite for folding of each monomer or the monomers must adopt some initial (correct) structure before correct assembly will occur. The "negative" mixing experiments between Phe8Gly cpn10 and wild-type cpn10 support the latter conclusion since, apparently, wild-type cpn10 cannot act as a template inducing structure in Phe8Gly cpn10.

The amino-acid sequences of the N- and C-terminal β-strands involved in subunit-subunit interactions in selected cpn10 proteins from various species have been aligned in Table 3 (residues 7 to 13 and 92 to 100 of the human cpn10 sequence). According to the SwissPROT database, there are 86 full-length sequences that show homology to cpn10. It is clear from the comparison of all these sequences that most of the subunit-subunit interface is conserved, at least with respect to the nature of each residue at each position. The interface in human cpn10 consists of mostly hydrophobic residues (of the 16 residues shown in Table 3; 11 are non-charged, mostly hydrophobic residues). Phenylalanine-8 in human cpn10 is conserved in 25 % of the compared species, but 100 % of the 86 sequences have an aliphatic, bulky residue (either Phe, Ile, Leu, or Val) at that position. The conservation of a large, hydrophobic residue at the position of phenylalanine-8 in all cpn10 species known suggests that it plays an important structural role in all cpn10 heptamers. In contrast, valine-100 is only conserved to 5 % in the 86 compared sequences. The presence of valine-100 at the interface in human cpn10 may therefore be to tune the interface plasticity so that cpn10 interactions with cpn60 and substrates are facilitated. Such interactions will be species specific, in accord with the variability of residues found at this position across the cpn10 family members.

Conclusions

It is not uncommon that point-mutations result in unfolded proteins. However, mutations that disrupt oligomeric unfolded states, like the two mutants characterized here, are unprecedented. Despite the large surface area and plasticity of the cpn10 monomer-monomer interface, our findings show that isolated residues can have crucial effects on the ability to assemble. Elimination of valine-100 does not affect the assembly in the folded state, but abolishes it in the unfolded state. However, elimination of phenylalanine-8 not only disrupts assembly in the unfolded state, but also the ability of the monomers to fold. Together with data on other interface mutants, these results may shed light on the unexpected observation of a heptameric unfolded state for wild-type cpn10 and the interplay between folding and assembly in a heptameric protein.

Methods

Preparation of human mitochondrial cpn10

Preparation of human cpn10 from recombinant *E. coli* has been described previously [24,25]. Protein concentration was determined from ε_{280} = 4200 $M^{-1}cm^{-1}$ (50 mM Tris-HCl, 135 mM NaCl, 6 M GuHCl) established by amino acid analysis.

Preparation of mutants

Design of the two mutants was performed by analysis of the crystal structure (see Results), selecting two residues at the interface. The QuickChange Site-Directed Mutagenesis Kit (Stratagene) was used to construct the selected point-mutated proteins. Briefly, plasmid constructs were subjected to multiple rounds of *de novo* DNA synthesis in the presence of mutagenic primers. Next, parental strands were digested with DpnI restriction enzyme, and potential

mutants were screened and sequenced to confirm mutations. Protein expression was performed by the stimulation of T7/Lac expression using pET24d plasmid (Novagen) constructs by addition of 2 mM IPTG (Promega). Purification of the cpn10 variants was carried out as previously described for wild-type cpn10. Yields of purified mutant proteins ranged from 15 to 45 mg per L cell culture.

Spectroscopic methods

Absorption spectra were measured on a Cary 50 spectrophotometer (1 cm cell). For far-UV circular dichroism (CD) measurements, an OLIS spectropolarimeter (1 cm cell for 1 to 5 μM cpn10; 1 mm cell for >5 μM cpn10; 200–260 nm spectra) was used. In CD measurements, the sample compartment was purged with nitrogen gas to avoid absorption by O_2. Fluorescence spectra (1 cm cell, excitation at 280 nm (tyrosine), emission maximum at 308 nm; 5 nm excitation and 5 nm emission slits, respectively) were collected on a Varian Eclipse fluorometer. Experiments were performed at 20°C in 5 mM phosphate buffer, pH 7, unless otherwise stated.

Cross-linking with gluteraldehyde

Reagents for cross-linking were purchased from Sigma. All cpn10 samples were prepared and incubated for ~10 min at 20°C before addition of gluteraldehyde (1 % w/v final). When needed, GuHCl was incorporated. After 2 min incubations, the reactions were quenched by addition of $NaBH_4$ (50 mM). Following 20 min further incubation, the cross-linked cpn10 solutions were precipitated with trichloroacetic acid (10 % w/v). The resulting pellets were analyzed by sodium dodecyl sulfate polyacrylamide gel electrophoresis (SDS-PAGE) using a pre-cast Novex gel (4–12 %) available from Invitrogen.

Gel-filtration

Gel filtration was performed on a calibrated 16/60 Superdex 75 column (Pharmacia). Calibration was performed with Pharmacia Low Molecular Weight Calibration Kit (Ribonuclease A, 13,700 Da; Chymotrypsinogen A, 25,000 Da; Ovalbumin, 43,000 Da; Bovine Serum Albumin, 67,000 Da; Blue Dextran 2000, » 2,000,000 Da). Due to its non-spherical shape, heptameric wild-type cpn10 runs as a 56,000 Da molecule under this calibration.

ANS binding

1-anilinonaphthalene-8-sulfonic acid (ANS) was purchased from Fluka (highest purity). ANS emission at 485 nm (excitation at 354 nm) was recorded for native conditions (buffer, pH 7, 20°C), and during heating, of wild-type and mutant cpn10 proteins in the presence of 25-fold molar excess ANS.

NMR spectra

NMR spectra were recorded on a Bruker Avance DRX 500 spectrometer in 5 mM phosphate buffer. The pH of the samples was adjusted with HCl. The spectrometer was equipped with a 5 mm Bruker inverse triple resonance probe with a triple axis gradient coil. In the 1D ^1H spectra water suppression was achieved using presat or watergate (3919) techniques [28].

Citrate synthase activity assay

The full procedure has been reported elsewhere [34], but the major steps are as follows. Pig-heart citrate synthase (Sigma) was denatured at room temperature for 20 minutes by dissolving solid GuHCl into a 40 mM solution of citrate synthase [3 mM DTT, 2 mM EDTA]. While vortexing, denatured citrate synthase was added to reaction mixtures of wild-type, Phe8Gly or Val100Gly cpn10 and *E. coli* GroEL. ATP was added to a final concentration of 2 mM to initiate chaperonin-assisted refolding. After 1 hour, an aliquot of the reaction was added to a quartz cell containing oxaloacetate, acetyl-CoA and phosphate buffer, pH 7.4. Citrate synthase activity (catalyzing the condensation of oxaloacetate and acetyl-CoA to citrate and CoA) was measured by the decrease in absorption at 233 nm, which corresponds to the disappearance of acetyl-CoA. The percent recovery of citrate synthase activity was normalized to the activity of the native protein.

Thermally-induced unfolding

Thermal unfolding was found to be reversible by far-UV CD and fluorescence and occurred in a single transition (midpoint corresponding to T_m) that was independent of detection method. Different equilibration times (5–10 minutes) at each temperature did not change the thermal profiles, and re-scans of original samples gave identical results with the exception of mixing experiments (see Results). Thermally-induced unfolding data for wild-type and Val100Gly cpn10 were collected at different protein concentrations (1–30 μM).

Thermally-induced unfolding was also monitored by DSC (MicroCal Inc.). Before start of such experiments, samples were degassed using a ThermoVac accessory unit. Prescan equilibration time was 30 minutes. At least three buffer-versus-buffer scans (25 to 85°C, 90°C/h) were taken to obtain a reproducible baseline. Every protein solution was scanned three times in order to assess reversibility of the reaction. The DSC scans were carried out under a pressure of 30 psi and passive (no cell-cell compensation) mode was used for the equilibration of reference and the sample cells. Protein concentration range was 50–100 μM and 5 mM phosphate buffer pH 6.0 was used in these experiments.

Chemically-induced unfolding

Chemical denaturants, urea (ICN Biochemicals) and GuHCl (Sigma Chemicals), were of highest purity. Urea solutions were prepared immediately before use. Unfolding of Val100Gly was monitored by far-UV CD and by fluorescence at various protein concentrations (see Results and Table 2). Stock solutions of urea or GuHCl were mixed with cpn10 solutions to give a fixed final protein concentration in each set of experiments. In all cases did far-UV CD and fluorescence give identical results. Equilibration time before measurements were 5–10 min. For unfolding of Val100Gly cpn10 in urea which was protein-concentration dependent, data analysis was performed using an apparent two-state reaction coupled to dissociation as described previously [26]. Unfolding of Val100Gly cpn10 in GuHCl was independent of the protein concentration and, therefore, each such transition was analyzed using a two state model without a dissociation [26]. Errors in thermodynamic parameters were derived from comparing multiple experiments.

Authors' Contributions

JJG carried out mutagenesis and biophysical experiments. FS carried out the GroEL-mediated refolding assay. KM and SL carried out the NMR studies. PWS conceived the study and participated in its design and coordination, she also drafted the manuscript. All authors read and approved the final manuscript.

Acknowledgements

The donors of the American Chemical Society Petroleum Research Fund (PWS), the National Science Foundation [MRI 9988269 (PWS and SL)], the National Institutes of Health [GM59663 (PWS)] are acknowledged for financial support. PWS is an Alfred P Sloan Research Fellow. We thank New Orleans Protein Folding InterGroup for valuable discussions.

References

1. Traut TW: *Crit Rev Biochem Mol Biol* 1994, **29:**125-63.
2. Darnall DW and Klotz IM: *Arch Biochem Biophys* 1975, **166:**651-82.
3. Bodenreider C, Kellershohn N, Goldberg ME and Mejean A: *Biochemistry* 2002, **41:**14988-99.
4. Ziegler MM, Goldberg ME, Chaffotte AF and Baldwin TO: *J Biol Chem* 1993, **268:**10760-5.
5. Mann CJ, Shao X and Matthews CR: *Biochemistry* 1995, **34:**14573-80.
6. Waldburger CD, Jonsson T and Sauer RT: *Proc Natl Acad Sci U S A* 1996, **93:**2629-34.
7. Nichtl A, Buchner J, Jaenicke R, Rudolph R and Scheibel T: *J Mol Biol* 1998, **282:**1083-91.
8. Gloss LM and Matthews CR: *Biochemistry* 1998, **37:**15990-9.
9. Doyle SM, Braswell EH and Teschke CM: *Biochemistry* 2000, **39:**11667-76.
10. Milla ME and Sauer RT: *Biochemistry* 1994, **33:**1125-33.
11. Srivastava AK and Sauer RT: *Biochemistry* 2000, **39:**8308-14.
12. Martin J, Geromanos S, Tempst P and Hartl FU: *Nature* 1993, **366:**279-82.
13. Todd MJ, Boudkin O, Freire E and Lorimer GH: *FEBS Lett* 1995, **359:**123-5.
14. Burston SG, Weissman JS, Farr GW, Fenton WA and Horwich AL: *Nature* 1996, **383:**96-9.
15. Shtilerman M, Lorimer GH and Englander SW: *Science* 1999, **284:**822-5.
16. Coates ARM: *The Chaperonins, Academic Press, London* 1996.
17. Cavanagh AC and Morton H: *Eur J Biochem* 1994, **222:**551-60.
18. Cavanagh AC: *Rev Reprod* 1996, **1:**28-32.
19. Hunt JF, Weaver AJ, Landry SJ, Gierasch L and Deisenhofer J: *Nature* 1996, **379:**37-45.
20. Mande SC, Mehra V, Bloom BR and Hol WG: *Science* 1996, **271:**203-7.
21. Roberts MM, Coker AR, Fossati G, Mascagni P, Coates AR and Wood SP: *Acta Crystallogr D Biol Crystallogr* 1999, **55:**910-4.
22. Hunt JF, van SM, der Vies, Henry L and Deisenhofer J: *Cell* 1997, **90:**361-71.
23. Hunt HLJ, Scott W, Guidry J, Landry S and Deisenhofer J: *PNAS* 2003 in press.
24. Landry SJ, Steede NK and Maskos K: *Biochemistry* 1997, **36:**10975-86.
25. Steede NK, Guidry JJ and Landry SJ: *Methods Mol Biol* 2000, **140:**145-51.
26. Guidry J, Moczygemba C, Steede K, Landry S and Wittung-Stafshede P: *Protein Sci* 2000, **9:**2109-2117.
27. Guidry JJ and Wittung P-Stafshede: *Arch Biochem Biophys* 2002, **405:**280-2.
28. Piotto M, Saudek V and Sklenar V: *J Biomol NMR* 1992, **2:**661-5.
29. Sirangelo I, Bismuto E, Tavassi S and Irace G: **.** *Biochim Biophys Acta* 1998, **1385:**69-77.
30. Cocco MJ and Lecomte JT: *Protein Sci* 1994, **3:**267-81.
31. Seale JW, Gorovits BM, Ybarra J and Horowitz PM: *Biochemistry* 1996, **35:**4079-83.
32. Fong DG, Doyle SM and Teschke CM: *Biochemistry* 1997, **36:**3971-80.
33. Wishart DS and Case DA: *Methods Enzymol* 2001, **338:**3-34.
34. Steede NK, Temkin S and Landry S: *Methods Mol Biol* 2000, **140:**133-38.

Publish with **BioMed Central** and every scientist can read your work free of charge

"BioMed Central will be the most significant development for disseminating the results of biomedical research in our lifetime."

Sir Paul Nurse, Cancer Research UK

Your research papers will be:

- available free of charge to the entire biomedical community
- peer reviewed and published immediately upon acceptance
- cited in PubMed and archived on PubMed Central
- yours — you keep the copyright

Submit your manuscript here:
http://www.biomedcentral.com/info/publishing_adv.asp

BioMedcentral